Bioresource Technology Reports 18 (2022) 101028

Contents lists available at ScienceDirect

Bioresource Technology Reports

journal homepage: www.sciencedirect.com/journal/bioresource-technology-reports

Real-time monitoring of biofilm thickness allows for determination of acetate limitations in bio-anodes

João Pereira [a,b], Siqi Pang [a], Casper Borsje [a], Tom Sleutels [a,c], Bert Hamelers [a], Annemiek ter Heijne [b,*]

[a] Wetsus, European Centre of Excellence for Sustainable Water Technology, Oostergoweg 9, 8911MA Leeuwarden, the Netherlands
[b] Environmental Technology, Wageningen University, Bornse Weilanden 9, P.O. Box 17, 6700 AA Wageningen, the Netherlands
[c] Faculty of Science and Engineering, University of Groningen, Nijenborgh 4, 9747 AG Groningen, the Netherlands

ARTICLE INFO

Keywords:
Bio-anodes
Acetate limitation
Maximum biofilm thickness
Identification model

ABSTRACT

Several studies have reported that current produced by electro-active bacteria (EAB) is dependent on anode potential and substrate concentration. However, information about the relation between biofilm growth and current density is scarce. In this study, biofilm thickness was monitored in-situ and this relation explored at three anode potentials and three acetate concentrations. The highest current densities of 3.7 $A{\cdot}m^{-2}$ were obtained for biofilms thinner than 40 μm, even though thicknesses up to 88 μm were measured. Fick's law was used to estimate the acetate penetration depth in the biofilm, acetate diffusion rates in the biofilm, and specific acetate utilization rates. A maximum biofilm thickness of a non-acetate limited biofilm of 55 μm and an acetate diffusion rate of 2.68×10^{-10} $m^2{\cdot}s^{-1}$ were estimated at −0.2 V vs Ag/AgCl. The results provide information on the target biofilm thickness for which no acetate limitations occur and provide data for modeling works with bio-anodes.

1. Introduction

Current production of bio-anodes in bio-electrochemical systems (BESs) depends on several parameters, such as reactor design, anode potential, substrate concentration and the amount of biomass present on the electrode (Borole et al., 2011; Guo et al., 2020; Hindatu et al., 2017). Since current production is catalyzed by electro-active bacteria (EAB), it is essential to determine the optimal set of parameters that lead to high amount of these bacteria in the biofilm developed on the anode surface.

The combination of more positive anode potentials and higher acetate concentrations has often been reported to stimulate growth of electro-active biofilms and results in higher current densities (Aelterman et al., 2008; Villano et al., 2016; Zhu et al., 2012). The difference between the anode potential and the acetate oxidation potential (overpotential) is a measure of the energy available for bacterial growth and maintenance, and as a result, the anode becomes more attractive as a surface to allow biomass growth when poised at higher overpotential. Regarding the acetate concentration, at low concentration, the current can be limited by acetate, while at higher concentrations, the current does not increase anymore as a function of concentration (Dhar and Lee, 2014; Sleutels et al., 2011). While the effect of anode potential and acetate concentration on current production has been subject of several studies, it is not known how biofilm thickness and current are related. On top of that, in continuous systems, the current has been observed to reach a maximum value already after a couple of days, after which it starts decreasing, most likely induced by certain limitations such as accumulation of protons in the biofilm due to acetate conversion (De Lichtervelde et al., 2019; Torres et al., 2010). So far, the effect of biofilm development has not been related to current production. Understanding the effect of biofilm thickness on current is important because it can help understanding limitations of bio-anodes and how to overcome those.

Real-time monitoring of biofilm thickness on the electrode is a challenging task due to the invasive characteristics of most techniques (Azeredo et al., 2017). Recently, a method has been developed to quantify the amount of electro-active biofilm, by using transparent Fluorine-doped Tin Oxide (FTO) electrodes (Molenaar et al., 2018). Optical Coherence Tomography (OCT) was used to scan the biofilm on the electrode, and the biofilm volume was determined. With OCT, it is thus possible to study the development of the biofilm on the anode real-time as a function of acetate concentration and anode potential.

Even though more current is produced when thicker biofilms are present on the electrode (Molenaar et al., 2018), too thick biofilms may

* Corresponding author at: Environmental Technology, Wageningen University, Bornse Weilanden 9, P.O. Box 17, 6700 AA Wageningen, the Netherlands.
E-mail address: annemiek.terheijne@wur.nl (A. ter Heijne).

https://doi.org/10.1016/j.biteb.2022.101028
Received 8 December 2021; Received in revised form 15 March 2022; Accepted 16 March 2022
Available online 23 March 2022

lead to mass transfer limitations of substrate, protons and buffer species between bulk solution and electrode surface. Ultimately, this may be reflected in decreasing current production as the biofilm grows thicker. On the one hand, being in direct contact with the electrode is an advantage since the resistance to transfer electrons is low, however, this comes at the expense of substrate availability. On the outer layers of the biofilm, facing the bulk solution, the microorganisms will have high acetate availability. However, the generated electrons after substrate oxidation need to pass a longer distance (higher resistance) to reach the electrode.

This trade-off between resistance for electron transfer and substrate availability in the biofilm suggests that the current produced per amount of total biofilm (commonly named specific microbial activity) will decrease when the biofilm grows so thick that limitations occur. Therefore, it is of crucial importance to define maximum biofilm thickness that guarantees access to acetate and avoid limitations in electron transfer. Measurement of biofilm growth over time under different conditions (substrate concentration and anode potential) allows understanding limiting factors and optimal thickness depending on these conditions and can provide information on specific biofilm activity. Moreover, these data can also be used to determine parameters, such as acetate diffusion in biofilms that are scarce in literature and need to commonly be assumed for modeling purposes.

In this study, the development of the biofilm was investigated on the anode surface at different anode potentials and acetate concentrations. Biomass growth was monitored real-time using Optical Coherence Tomography (OCT). Based on the combination of a continuous monitoring of biofilm growth on the electrode and the produced current, a model that identifies acetate limitations in the biofilm was developed. This model was used to estimate the thickness of a biofilm through which acetate can penetrate completely, at three acetate concentrations and three anode potentials, and it was used to calculate acetate diffusion rates inside electro-active biofilms and specific acetate utilization rates of EAB.

2. Materials and methods

2.1. Experimental setup and reactor configuration

The experiments were performed with the electrochemical cells previously described by Molenaar et al., 2018. These reactors were composed of two flow compartments: an anode and a cathode (each with a volume of 33 cm^3). Between these compartments, a bipolar membrane (Ralex PEBPM, MEGA a.s., Czech Republic) was placed with the anion side facing the anode and the cation side facing the cathode to keep the pH in the anode stable. To allow real time monitoring of the biofilm development, a transparent Fluorine-doped Tin Oxide (FTO) coated glass electrode was used as anode. Graphite sheet was placed in contact with the FTO electrode (around its operating area of 22.3 cm^2) to work as current collector. In the cathode compartment, a flat platinum/iridium coated titanium plate (Pt/IrO2 80:20, Magneto special anodes BV, Schiedam, The Netherlands) was used as counter electrode.

The anode compartment was continuously fed with influent at a rate of 0.36 $mL{\cdot}min^{-1}$, while both anolyte (stream present in the anode compartment of the reactor) and catholyte (stream present in the cathode compartment of the reactor) were continuously recirculated at 60 $mL{\cdot}min^{-1}$ (Masterflex L/S, Cole-Parmer, Barendrecht, The Netherlands). The anode compartments were operated with a hydraulic retention time of 10 h (volume of anolyte of 220 mL), while the cathode compartments were operated in batch (i.e. without inflow of fresh catholyte nor outflow of catholyte). The reactors were electrically connected to a potentiostat (N-stat d-module, Ivium Technologies, Eindhoven, The Netherlands) that was used to control the anode potential. Reference electrodes were positioned in between the FTO electrode and the bipolar membrane by means of Haber–Luggin capillaries filled with 3 M KCl solution. All potentials are expressed using an Ag/AgCl electrode (+0.203 V vs. Standard Hydrogen Electrode; Prosense, Oosterhout, The Netherlands), and the current produced by each bio-anode was recorded every minute. The reactors were operated at 298 K in a temperature-controlled cabinet. To avoid oxygen penetration in the reactors during sampling in the OCT, Quick-Coupler valves (Swagelok SS-QC4-D-400, USA) were used.

2.2. Inoculum and electrolyte composition

A mixture of acetate fed biomass from active bio-anodes was used as inoculum in all experiments. The influent was prepared according to DSMZ culture medium 141 and it constituted of ($g{\cdot}L^{-1}$): 0.04, 0.17, and 0.65 $NaCH_3COO$, 3.40 KH_2PO_4, 4.36 K_2HPO_4, 0.1 $MgSO_4.7H_2O$, 0.74 KCl, 0.58 NaCl, 0.28 NH_4Cl, 0.1 $CaCl_2.2H_2O$, 1 mL of trace metals mixture and 1 mL of vitamins mixture (DSMZ, 2017). Sodium 2-bromoethanesulfonate (1.97 $g{\cdot}L^{-1}$) was added to the influent to inhibit methanogenesis. Anaerobic conditions in the reactor were maintained by continuously sparging the influent with nitrogen before and during the experiments. The catholyte consisted of 50 mM phosphate buffer solution at pH 7. Nitrogen was continuously sparged into the catholyte recirculation vessel during operation to avoid accumulation of hydrogen and possible diffusion towards the anode.

2.3. Experimental strategy

The influence of anode potential and different acetate concentrations on electro-active biofilm growth was studied based on 126 experimental runs. Each reactor operated for at least 10 days and each condition was tested in duplicate. All the data points of each experiment are shown. This approach was chosen as all the trends of the data are shown and it provides the most information for the modeling. Acetate concentrations of 0.5, 2 and 8 mM were used in the influent, with the aim to include limiting, average, and high acetate concentrations. The anode potential was controlled at −0.2, −0.3 and −0.4 V vs Ag/AgCl. Considering the thermodynamic acetate oxidation potential at biological standard conditions of −496 mV vs Ag/AgCl (Logan et al., 2006), these are low overpotentials and only up to 0.3 V will be available for cell growth and maintenance. However, this range of low anode potentials was selected to represent conditions in which reasonable voltage efficiency can be achieved in a Microbial Fuel Cell.

2.4. Acetate consumption and online monitoring of biofilm growth

Acetate concentration was measured using Ultra-High-Performance Liquid Chromatography (UHPLC) (300 × 7.8 mm Phenomenex Rezex Organic Acid H+ column, Dionex ultimate 3000RS, Thermo Fisher Scientific, The Netherlands) after filtration of samples through a 0.45 μm pore-size filter (EMD Millipore SLFH025NS, Barendrecht, The Netherlands) (Lee et al., 2009). Consumed acetate ($Ac_{consumed}$, mol) was calculated as described in Eq. (1), in which Ac_{in} (mM) is the acetate concentration in the influent, Ac_{out} (mM) is the acetate concentration in the anolyte, *flow* is the flowrate ($mL{\cdot}min^{-1}$) and Δt (min) is the time between samples.

$$Ac_{consumed} = (Ac_{in} - Ac_{out}) \times flow \times \Delta t \quad (1)$$

Optical Coherence Tomography (OCT) was used to monitor the biofilm growth on the anode in real time (Molenaar et al., 2018). For OCT measurements, the reactors were disconnected hydraulically and electrically and placed on the OCT visualization stage. The electrode was then scanned at 54 evenly distributed spots, to allow for accurate imaging of the amount of the biofilm on the electrode within reasonable measuring duration. The OCT measurements took approximately 45 min, and no significant changes in acetate concentration nor produced current before and after the measurements were observed. The scans of the electrode with biofilms were run in a MATLAB script that isolated and counted the pixels corresponding to biofilm. The resulting number

of pixels was converted to biomass weight (mg COD) using the calibration line reported (Molenaar et al., 2018). Biofilm thickness (in μm) was determined after dividing the average volume of each biofilm by the area of the electrode. Due to the detection limit of the OCT, biofilms thicknesses thinner than 5 μm were not considered. Since different anode potentials and acetate concentrations were used in this study when compared to the operating conditions used by Molenaar et al., 2018, COD measurements of the biofilms were performed on the last day and confirmed that the calibration curve was valid. Both acetate analysis and OCT measurements were performed every two or three days throughout each experiment.

2.5. Basic model to identify acetate limitation in biofilms

A basic model to identify acetate limitation in the biofilms was used. This model was used to calculate the penetration depth of acetate inside the biofilm based on Fick's law (Eq. (2)), where $L_{acetate}$ is the penetration depth (m), D_s is the diffusion of acetate in the biofilm ($m^2 \cdot s^{-1}$), Ac_{out} is the acetate concentration in the anolyte (mol $Ac \cdot m^{-3}$) and, k_0 is the specific acetate utilization rate (mol $Ac \cdot m^{-3} \cdot s^{-1}$).

$$L_{acetate} = \sqrt{[(2 \times D_s \times Ac_{out})/k_0]} \quad (2)$$

Measured concentrations of acetate in the anolyte and measured biofilm thicknesses were used as input. Based on these, the model was used to estimate the penetration depth of acetate, acetate diffusion and specific acetate utilization rate. In addition, using the specific acetate utilization rate, an estimated current density based on substrate availability was calculated that was compared with the measured current density. The estimated current density was calculated according to Eq. (3):

$$j_{estimated} = L_{minimum} \times k_0 \quad (3)$$

where $j_{estimated}$ represents the current density estimated by the model (mol $Ac \cdot m^{-2} \cdot s^{-1}$) and $L_{minimum}$ is the minimum biofilm thickness, which is the lowest thickness when comparing the estimated acetate penetration depth, or the measured biofilm thickness. The specific acetate utilization rate was used to estimate the current density (in mol $Ac \cdot m^{-2} \cdot s^{-1}$) assuming a 100% Coulombic efficiency, which is realistic since the Coulombic efficiencies obtained for all bio-anodes were high (above 90%).

The three parameters of interest: $L_{acetate}$, D_s and k_0 were determined using minimization of the sum of squares between the estimated and the experimental current densities. This approach was used for the 126 experimental data points that constitute the dataset of this study. The data were grouped for anode potential and the three parameters were estimated. More details on the model can be found in the Supplementary data.

3. Results and discussion

3.1. Higher acetate concentrations lead to higher current at the bio-anode

Fig. 1.a shows the relation between the measured current density and the acetate concentration in the anolyte, based on the 126 measurements performed for all experiments together. Overall, an increase in acetate concentration resulted in higher current density. A maximum current density of 3.7 $A \cdot m^{-2}$ was obtained when the bio-anode was fed with 8 mM acetate. The influence of anode potential on current produced and acetate consumed is also depicted in Fig. 1. More acetate was consumed when the anode was controlled at −0.2 and −0.3 V, resulting in higher current densities (approximately 2 mM of acetate was consumed at −0.2 V and 1.5 mM at −0.3 V, both determined when the anode was fed with 8 mM acetate). Overall, these results show that the current produced by EABs is mainly limited by the anode potential when controlled at −0.4 V, since similar current densities were obtained when the bio-anode was fed with 2 and 8 mM. Nevertheless, current produced is mainly limited by the acetate concentration when the anode potential is controlled at −0.2 and −0.3 V, since similar current densities at these two anode potentials were obtained when the bio-anode was fed the same acetate concentration.

The relation between the measured concentration of acetate and the calculated acetate concentration in the anolyte based on current produced shows that the Coulombic efficiency was close to 100% in all experiments (Fig. 1.b). Since the current produced relates to the acetate consumption, this confirms that acetate was consumed by electro-active microorganisms. Therefore, competitive processes in the anode such as the presence of methanogens and sulphur reducers are neglected, making this experimental setup suitable to study electro-active biofilms.

3.2. Current density reaches a maximum at biofilm thickness between 10 and 30 μm and decreases when biofilms grow thicker

The current profiles as a function of time were similar for all the bio-

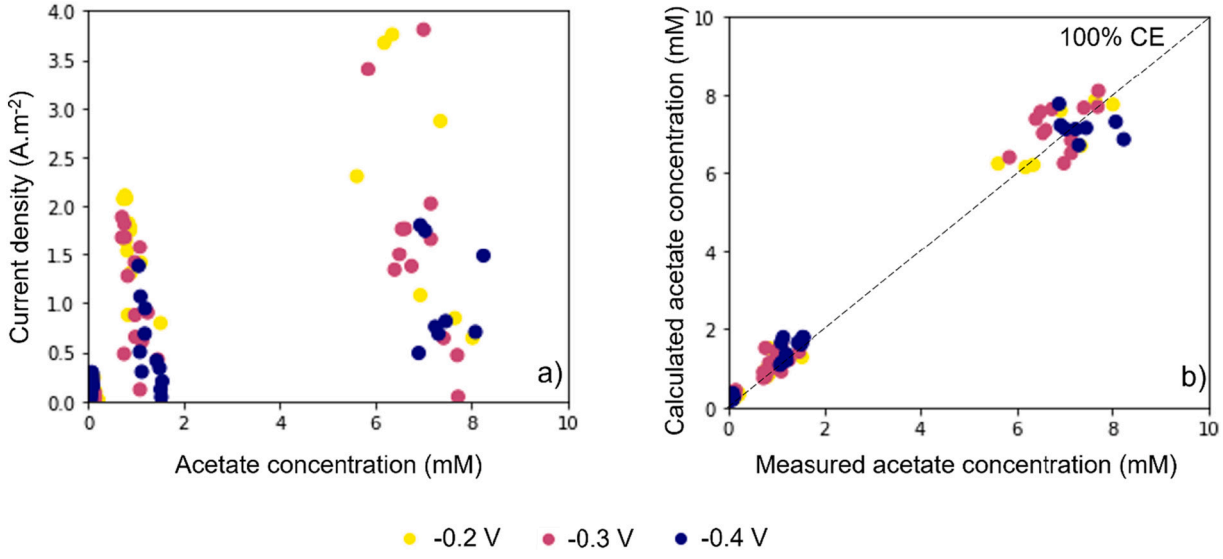

Fig. 1. (a) Current produced as a function of the acetate concentration in the anolyte for −0.4, −0.3 and −0.2 V vs Ag/AgCl, and (b) relation between measured and calculated acetate concentration in the anolyte shows that Coulombic efficiency was close to 100% (dashed line) for all data points.

anodes (in Supplementary data): for all experiments, the current reached a peak, after which it flattened out or decreased, while the biofilm thickness increases with time, and keeps increasing also after a maximum in current is reached. Fig. 2 shows the current density produced by the biofilm on the electrode for all the conditions applied. Generally, the maximum current density was reached at biofilm thicknesses in the range of 10–30 μm. When biofilm thickness increases beyond 30 μm, the current does not further increase and in most cases decreases. Nevertheless, a high current density was obtained when the biofilm thickness was approximately 47 μm (at −0.3 V vs Ag/AgCl). The reason for this high acetate conversion cannot be explained with the measured parameters that constitute the dataset of this study.

When the bio-anode was fed with 0.5 mM acetate, current densities were lower than 0.5 $A{\cdot}m^{-2}$ and the maximum biofilm thickness was 25 μm (at −0.3 V). At this acetate concentration, increasing the anode potential did not have an effect on current density (Fig. 2.b and c). This indicates that the current production was determined by acetate availability at the lowest acetate concentration. Increasing the influent acetate concentration to 2 mM resulted in current densities varying between 1.0 and 2.0 $A{\cdot}m^{-2}$. The biofilm thickness ranged between 5 and 25 μm at −0.4 V (Fig. 2.a), and thicker biofilms were found for more positive anode potentials, reaching a maximum of 55 μm at −0.3 V and 78 μm at −0.2 V. However, this increase in biofilm thickness did not result in a higher current. Feeding the bio-anode with 8 mM acetate (highest acetate concentration) resulted in the highest current densities of approximately 3.7 $A{\cdot}m^{-2}$. These current densities were obtained at −0.3 V when the biofilm was 10 μm thick (Fig. 2.b), and at −0.2 V when the biofilm was 25–30 μm thick (Fig. 2.c). Even though increasing the anode potential from −0.4 to −0.3 V resulted in a steep increase in current density, when the potential was further increased from −0.3 to −0.2 V, there was no clear increase in current density. The thickest biofilm at −0.4 V was 88 μm, 65 μm at −0.3 V, both measured when 8 mM acetate was used whereas the thickest biofilm at −0.2 V was 78 μm when 2 mM acetate was used.

The current densities obtained are comparable to previously reported current densities ranges obtained with flat and non-capacitive electrodes. With a similar reactor design, Molenaar et al., 2018 reported maximum current densities up to 2 $A{\cdot}m^{-2}$ followed by a decrease to approximately 1 $A{\cdot}m^{-2}$ when the anode was fed with 10 mM acetate and the anode potential controlled at −0.35 V. Under the same operating conditions and with an circular FTO electrode, ter Heijne et al. (2018) reported a maximum current of 0.7 $A{\cdot}m^{-2}$ and 1.1 $A{\cdot}m^{-2}$. These results are also in accordance with previous studies that reported higher currents when higher anode potentials and non-limiting acetate concentrations were used (Sleutels et al., 2011, 2016).

3.3. *Identifying acetate limitations via penetration depth in bio-anodes*

The biofilm thicknesses of 18 experiments were measured in 126 measurements, and the measured biofilm thicknesses ranged between 5 and 88 μm. Generally, for biofilm thicknesses up to about 30 μm, thicker biofilms resulted in higher current density. Further growth of the biofilm resulted in stable or decreasing currents. Since the biofilm continued growing when the current leveled off and/or decreased, the specific bio-electrocatalytic activity of the bio-anodes, i.e. the current produced per amount of biofilm, decreased for thicker biofilms. At early stages of biofilm growth, the highest specific bio-electrocatalytic activity was found for the most positive anode potential of −0.2 V in combination with the highest acetate concentration of 8 mM, for biofilms thinner than 30 μm. The highest specific bio-electrocatalytic activity was 2.5 $A{\cdot}g_{COD}^{-1}$. When the biofilms grew thicker, specific activities decreased to 0.2–0.5 $A{\cdot}g_{COD}^{-1}$ for all anode potentials and acetate concentrations tested.

Even though biofilm growth is always linked to current produced, two different relations between growth and current can be defined. During early-stage growth, the measured increase in biofilm thickness is

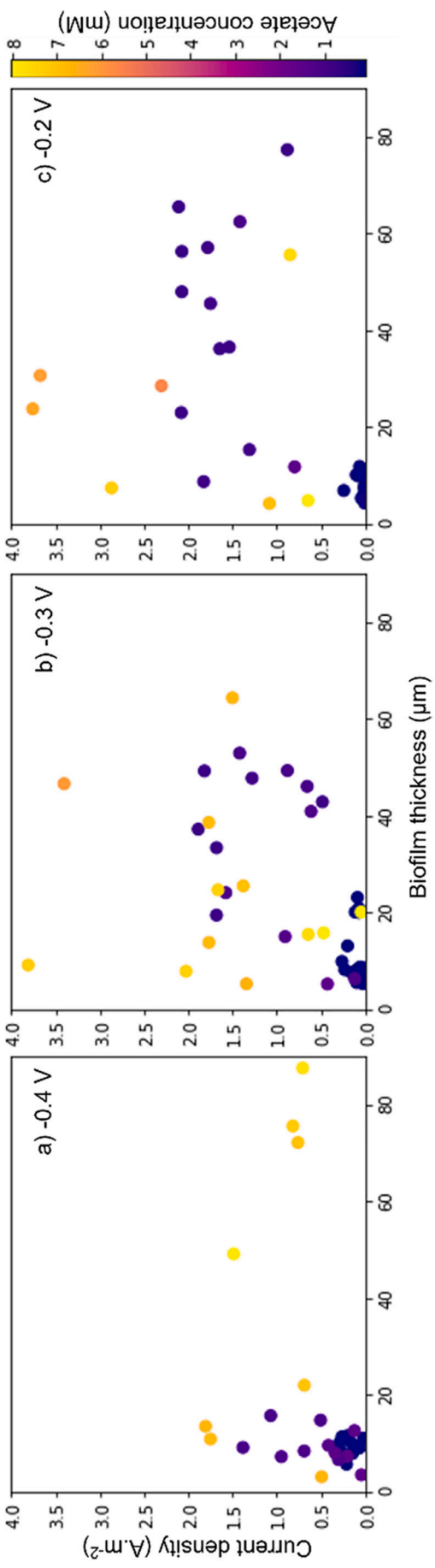

Fig. 2. Current density profiles as a function of the biofilm thickness when the anode was poised at a) −0.4 V, b) −0.3 V and c) −0.2 V (vs Ag/AgCl). Current reached a maximum at biofilm thickness between 10 and 30 μm, while at higher biofilm thickness, current decreased.

related to increase in current density. This relation between biofilm thickness and current is characteristic for the low range of biofilm thicknesses (up to approximately 30 μm), in which the highest specific activities are obtained as long as current is not limited by substrate availability and anode potential. When biofilms grow further, current produced flattens out or decreases, shifting the relation between biofilm thickness and current produced. In this stage, characterized by lower specific microbial activities, there is growth and accumulation of biomass that results in an overall decrease on the rate of electrons transfer to the anode. This decrease in specific bio-electrocatalytic activity could be caused by diffusion limitations in the biofilm that creates an additional resistance for the electrons to flow towards the electrode as well as mass transfer limitations of acetate and/or products (Renslow et al., 2013; ter Heijne et al., 2015). Thus, the biofilm as a whole becomes less electro-active.

3.4. Ratio of electro-active biofilm on the electrode increases with higher acetate concentration and more positive anode potential

The shift in the relation between the current density and the thickness of the biofilm on the anode indicates that bacteria slow down the rate of electrons transferred to the electrode when biofilm grows thicker. The measurements obtained on real-time biofilm thickness can be used to better understand diffusion limitations in the bio-anode and to determine the optimal biofilm thickness depending on the conditions applied (anode potential and acetate concentration). The acetate penetration depths in the biofilm was selected as the most limiting factor, since the availability of acetate showed to be more determinant for the current density of bio-anodes than the anode potential applied (as shown in Fig. 2 and mentioned in the previous sections). The concentration of acetate and the biofilm thickness (distance to the electrode) are intrinsically related parameters determining the produced current. If the availability of the carbon source is not evenly distributed over the depth of the biofilm, the bacteria experiencing low acetate concentration will oxidize less acetate and, therefore, produce lower current at the electrode than bacteria experiences higher acetate concentrations. Moreover, as the biofilm grows further away from the electrode, the losses to use the electrode as electron acceptor become bigger.

By calculating the acetate penetration depth into the biofilm at different conditions, the biofilm thickness that is non-acetate limited, and that is therefore able to contribute to the produced current, can be determined. Fig. 3 shows the ratio between non-acetate limited biofilm and the total biofilm measured on the FTO electrode as a function of the measured biofilm thickness. Ratios of 1 are obtained when acetate penetrates the whole biofilm, i.e. the biofilm activity is not limited by acetate supply. Ratios below 1 show which part of the biofilm has access to acetate: for example, a ratio of 0.6 means that acetate penetrates 60% of the measured biofilm thickness and the remaining 40% of the biofilm has no acetate.

In general, the thickness of a non-acetate limited biofilm increases with higher acetate concentrations and more positive anode potentials. At low acetate concentrations, only part of the biofilm will have access to acetate, and most of the data points show a ratio <1. For the highest acetate concentrations, a ratio of non-acetate limited biofilm over total biofilm of 1 is found, meaning that the whole biofilm has access to acetate, until a certain biofilm thickness is reached, and after that the ratio goes down. A maximum thickness of 55 μm was calculated for biofilms fed with 8 mM acetate and with the anode potential controlled at −0.2 V. At the same concentration, the thickness of the biofilms that faced no acetate diffusion limitations decreased to 39 μm when the anode potential was poised at −0.3 V, and to 11 μm at −0.4 V. At lower acetate concentrations, the penetration depth of acetate is smaller: for 0.5 mM acetate in the influent, a maximum biofilm thickness of 10 μm was obtained, while for 2 mM acetate in the influent, a maximum biofilm thickness of 24 μm was obtained, both at −0.2 V. Particularly for the bio-anodes fed with 0.5 mM acetate (the lowest acetate concentration), a

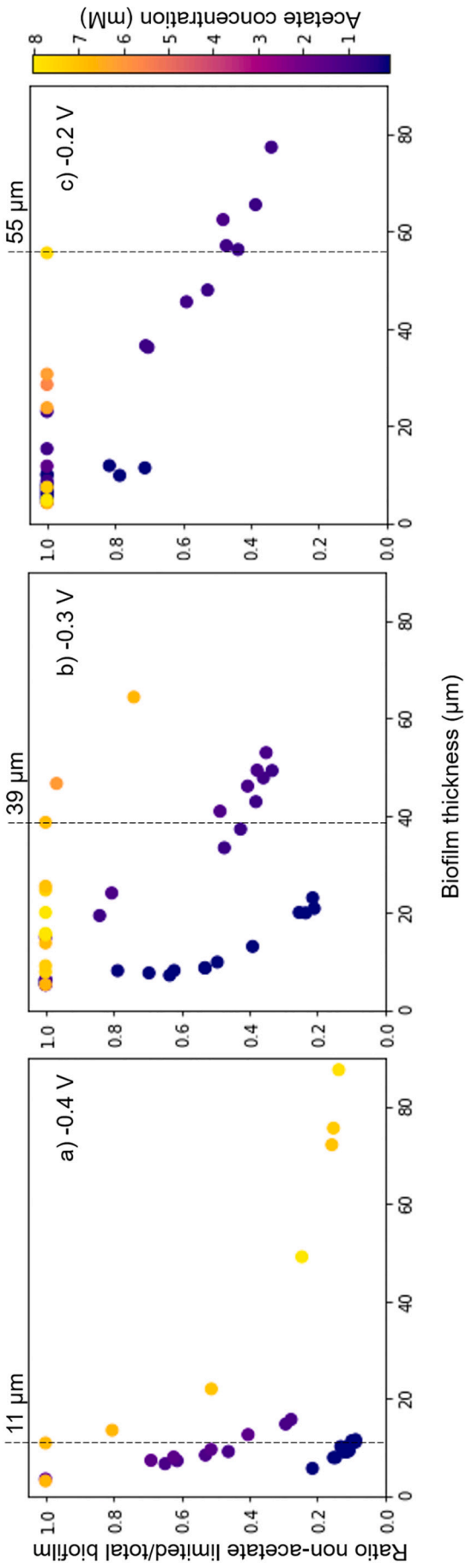

Fig. 3. Ratio between non-acetate limited biofilm and total biofilm measured with OCT as a function of the biofilm thickness when the anode was poised at a) −0.4 V, b) −0.3 V and c) −0.2 V (vs Ag/AgCl).

steep increase in acetate-limited biomass was observed within a few micrometers of biofilm thickness, indicating that extremely low acetate concentrations 1) do not allow an efficient penetration of acetate in the biofilm, and 2) do not result in growth of thick biofilms.

Although very limited studies have been performed, the limiting biofilm thicknesses determined based on the acetate penetration depth are in line with other findings. For example, the CLSM study on bio-anodes reported by Sun et al. (2016) reported an increasing microbial activity until a biofilm thickness of 20 μm in a bio-anode fed with 16 mM acetate. They reported a decrease in activity for a 45 μm thick biofilm that was associated to the presence of a dead layer of bacteria in direct contact with the electrode (Sun et al., 2017). In another studies, a biofilm thickness of 50 μm has been reported to guarantee a thoroughly electro-active biofilm and limitations in produced current were encountered at biofilm thicknesses ranging 40 and 60 μm (Franks et al., 2010, 2012; Ly et al., 2013). Biofilm thicknesses in the range of 4 to 58 μm have been reported in study on the effect of shear stress on bio-anodes, and biofilms thicker than 68 μm has been measured on a study focused on the effect of pH and buffer concentration on current produced at the anode (Lusk et al., 2016; Pham et al., 2008).

Even though thicker biofilms grew on the FTO electrode with higher acetate concentrations and more positive anode potentials, it is essential to highlight that large parts of these biofilms were not accessible to acetate (60–90%). These were the biofilms that produced the lowest current densities (Supplementary data). Even though these acetate limited biofilms (ratio lower than 1) produced current densities up to 2 $A{\cdot}m^{-2}$, only non-acetate limited biofilms (ratios equal to 1) produced higher current densities. The analysis of the ratio of non-acetate limited biomass indicates the operating conditions and the thicknesses at which the biofilm should be controlled to guarantee and maintain high current densities. This is of crucial importance in practical applications since higher current production is related to maximum acetate conversion, which can only be obtained in non-acetate limited biofilms. Therefore, strategies to keep the biofilm thickness within the non-limiting range of thicknesses, by means of sheer stress or scraping off the top layers of the biofilm must be taken into account when developing microbial electrochemical technologies for practical applications.

In practical applications with real wastewaters, the thicknesses of a non-acetate limited electro-active biofilm are expected to be slightly thinner than the thicknesses reported in this study. Given the complexity of real wastewaters streams that include the presence of several microbial species and alternative electron donors and acceptors, it is likely that other species will thrive in the biofilm and competing processes for acetate will happen (Sleutels et al., 2016). Nevertheless, in the research field, the reported optimal range of biofilm thicknesses and acetate limitations can give fruitful insights on bio-cathodes. Even though bio-cathodes have an opposed working principle to bio-anodes (in the sense that energy is consumed to produce chemical compounds, and consumption of electrons is related to consumption of protons), limitations due to the distance to the cathode (electron donor) and the accumulation of products (acetate or other long chain fatty acids such as caproate) will also create limitations in the biofilm. The results reported here for electro-active biofilms on an anode cannot be directly extrapolated to the growth of electro-active biofilms on a cathode, given the different substrates and product and microbial community of the biofilms. However, applying a similar methodology on bio-cathodes to measure and monitor their thickness over time can reveal the optimal operating range and give insights on how to optimize their performance.

3.5. Practical acetate diffusion and specific acetate utilization rates in electro-active biofilms

Two parameters were derived from Fick's equation: the acetate diffusion rate, D_s, and the specific acetate utilization rate, k_0. These are essential parameters to characterize any bioprocess as they allow for a better understanding and for a more accurate description and control of processes. In bio-anode studies, these parameters are often needed for modeling purposes and assumed values are used since no experimental data are available. With the extended dataset on biofilm thicknesses and concentrations of acetate, practical diffusion rates of acetate in biofilms and specific acetate utilization rate at three different anode potentials can be estimated (Table 1). Even though these parameters are not directly linked to the applied anode potential, more understanding on structural and compositional differences in the electro-active biofilms can be obtained when deriving these parameters for each anode potential tested in this study. Acetate diffusion rates are also influenced by factors other than the acetate concentration in the anolyte. These factors include structural and compositional characteristics and viability of the biofilm. When denser biofilms grow on the electrode (i.e. less porous and more cellular packed biofilm structures), lower acetate diffusions rates are expected. Acetate penetration can also be hindered by the presence of a more solid extracellular matrix composed of saturated lipids and less flexible polysaccharides and proteins structures. Finally, lower acetate diffusion rates are expected to be obtained if biofilms were mainly composed of dead biomass.

Acetate diffusion rates in the order of 1×10^{-10} $m^2{\cdot}s^{-1}$ were obtained when the anode potential was −0.3 and −0.2 V, and 1×10^{-11} $m^2{\cdot}s^{-1}$ when the anode potential was −0.4 V. These diffusion rates are slightly lower than those typically reported for diffusion rates (10^{-9} $m^2{\cdot}s^{-1}$ in water). Since the acetate diffusion rates are here calculated inside the biofilm structure, where mass transfer resistance is higher than when acetate diffuses in water, it is not surprising that the rates are one order of magnitude lower.

The diffusion of acetate in the biofilm increased with more positive anode potentials (1.02×10^{-11} $m^2{\cdot}s^{-1}$ at −0.4 V, 1.09×10^{-10} at −0.3 V and 2.68×10^{-10} $m^2{\cdot}s^{-1}$ at −0.2 V). For the more positive anode potentials, acetate diffusion rates similar to the values commonly assumed in literature were obtained. Korth et al., 2015 assumed an acetate diffusion rate in biofilms of 5.5×10^{-10} $m^2{\cdot}s^{-1}$ after using a 0.5 correction factor from the acetate diffusion in water (1.1×10^{-9} $m^2{\cdot}s^{-1}$), whereas Marcus et al., 2007 assumed 8.7×10^{-10} $m^2{\cdot}s^{-1}$ after using a reduction factor of 0.8 (Wanner et al., 2006) on the acetate diffusion rate in water reported in Lide, 2006. More acetate diffusion values have been assumed in other studies (Renslow et al., 2013; Wanner and Gujer, 1986). With the outcomes of the model, realistic acetate diffusion rates in biofilms at three different anode potentials are provided and can be used for future modeling work in electro-active biofilms.

The model also predicts specific acetate utilization rates. This parameter is a measure of the maximum acetate converted (so-called maximum activity) by EAB. Specific acetate utilization rates of 0.08 mol $Ac{\cdot}m^{-3}{\cdot}s^{-1}$ were obtained at −0.3 and − 0.2 V and a higher specific acetate utilization rate of 0.14 mol $Ac{\cdot}m^{-3}{\cdot}s^{-1}$ was obtained at −0.4 V. These results corroborate with data previously reported for EAB. For example, Marcus et al., 2007 used a maximum acetate utilization of mol 0.08 mol $Ac{\cdot}m^{-3}{\cdot}s^{-1}$ and Lee et al., 2009 reported a maximum acetate utilization of 0.20 mol $Ac{\cdot}m^{-3}{\cdot}s^{-1}$ (biomass density of 50 kg $VS{\cdot}m^{-3}$ (Lee et al., 2009) was used to convert the reported activities of 0.132 mmol $Ac{\cdot}mg\ VS^{-1}{\cdot}d^{-1}$ and 22.3 kg $COD{\cdot}kg\ VS^{-1}{\cdot}d^{-1}$, respectively). When compared to anaerobic digesters that usually use as rule of thumb a conversion of 2 kg $COD{\cdot}kg\ VS^{-1}{\cdot}d^{-1}$ (Arends and Verstraete, 2012) (approximately 0.02 mol $Ac{\cdot}m^{-3}{\cdot}s^{-1}$ considering a biomass density of 50 kg $VS{\cdot}m^{-3}$), these results show comparable specific acetate

Table 1
Acetate diffusion rate and specific acetate utilization rate in electro-active biofilms as a function of the anode potential (all anode potentials are expressed vs Ag/AgCl).

Parameters	E = − 0.4 V	E = − 0.3 V	E = − 0.2 V
D_s ($m^2{\cdot}s^{-1}$)	1.02×10^{-11}	1.09×10^{-10}	2.68×10^{-10}
k_0 (mol $Ac{\cdot}m^{-3}{\cdot}s^{-1}$)	0.14	0.08	0.08

utilization rates for EAB. However, tailoring biofilm thicknesses to avoid acetate limitation and optimize acetate conversion rates by EAB is essential, especially when the higher operating rates reported in anaerobic digesters need to be achieved (5–25 kg COD·kg VS^{-1}·d^{-1}) (Pham et al., 2006).

4. Conclusion

Bio-anodes must be operated in a way that the highest current is achieved with a thin electro-active biofilm. This requires a controlled biomass development on the electrode up to a certain thickness to guarantee acetate availability inside the biofilm and to ensure high electron transfer rates to the electrode. Therefore, growing thin biofilms and managing the biomass thickness on the electrode to suit the operating conditions is essential to maintain higher current densities, and it serves as a strategy to narrow down the limiting variables towards a better understanding of other possible limiting phenomena occurring in the EAB.

Funding

This work was supported by the “Resource Recovery” theme of Wetsus and Dutch Research Council (NWO) [project “Understanding and controlling electron flows in electro-active biofilms” with project number 17516 that is part of the research programme Vidi].

CRediT authorship contribution statement

João Pereira: Conceptualization, Methodology, Investigation, Writing – original draft. **Siqi Pang:** Methodology, Validation. **Casper Borsje:** Methodology, Investigation. **Tom Sleutels:** Conceptualization, Writing – review & editing. **Bert Hamelers:** Conceptualization, Writing – review & editing. **Annemiek ter Heijne:** Conceptualization, Writing – review & editing, Supervision, Project administration, Funding acquisition.

Declaration of competing interest

The authors declare that they have no known competing financial interests or personal relationships that could have appeared to influence the work reported in this paper.

Acknowledgements

This work was performed in the cooperation framework of Wetsus, European Centre of Excellence for Sustainable Water Technology (www.wetsus.nl). Wetsus is co-funded by the Dutch Ministry of Economic Affairs and Ministry of Infrastructure and Environment, the European Union Regional Development Fund, the Province of Fryslân, and the Northern Netherlands Provinces. The authors thank the participants of the research theme “Resource Recovery” for the fruitful discussions and their financial support. This publication is part of the project “Understanding and controlling electron flows in electro-active biofilms” with project number 17516 of the research programme Vidi which is (partly) financed by the Dutch Research Council (NWO).

Appendix A. Supplementary data

Supplementary data to this article can be found online at https://doi.org/10.1016/j.biteb.2022.101028.

References

Aelterman, P., Freguia, S., Keller, J., Verstraete, W., Rabaey, K., 2008. The anode potential regulates bacterial activity in microbial fuel cells. Appl. Microbiol. Biotechnol. 78, 409–418. https://doi.org/10.1007/s00253-007-1327-8.

Arends, J.B.A., Verstraete, W., 2012. 100 years of microbial electricity production: three concepts for the future. Microb. Biotechnol. https://doi.org/10.1111/j.1751-7915.2011.00302.x.

Azeredo, J., Azevedo, N.F., Briandet, R., Cerca, N., Coenye, T., Costa, A.R., Desvaux, M., Di Bonaventura, G., Hébraud, M., Jaglic, Z., Kačániová, M., Knøchel, S., Lourenço, A., Mergulhão, F., Meyer, R.L., Nychas, G., Simões, M., Tresse, O., Sternberg, C., 2017. Critical review on biofilm methods. Crit. Rev. Microbiol. 43, 313–351. https://doi.org/10.1080/1040841X.2016.1208146.

Borole, A.P., Reguera, G., Ringeisen, B., Wang, Z.W., Feng, Y., Kim, B.H., 2011. Electroactive biofilms: current status and future research needs. Energy Environ. Sci. 4, 4813–4834. https://doi.org/10.1039/c1ee02511b.

De Lichtervelde, A.C.L., Ter Heijne, A., Hamelers, H.V.M., Biesheuvel, P.M., Dykstra, J. E., 2019. Theory of ion and electron transport coupled with biochemical conversions in an electroactive biofilm. Phys. Rev. Appl. 12, 1. https://doi.org/10.1103/PhysRevApplied.12.014018.

Dhar, B.R., Lee, H.S., 2014. Evaluation of limiting factors for current density in microbial electrochemical cells (MXCs) treating domestic wastewater. Biotechnol. Rep. 4, 80–85. https://doi.org/10.1016/j.btre.2014.09.005.

DSMZ, 2017. 141. Methanogenium medium (H2/CO2) [WWW document]. URL https://www.dsmz.de/microorgan- isms/medium/pdf/DSMZ_Medium141.pdf.

Franks, A.E., Nevin, K.P., Glaven, R.H., Lovley, D.R., 2010. Microtoming coupled to microarray analysis to evaluate the spatial metabolic status of Geobacter sulfurreducens biofilms. ISME J. 4, 509–519. https://doi.org/10.1038/ismej.2009.137.

Franks, A.E., Glaven, R.H., Lovley, D.R., 2012. Real-time spatial gene expression analysis within current-producing biofilms. ChemSusChem 5, 1092–1098. https://doi.org/10.1002/cssc.201100714.

Guo, Y., Rosa, L.F.M., Müller, S., Harnisch, F., 2020. Monitoring stratification of anode biofilms in bioelectrochemical laminar flow reactors using flow cytometry. Environ. Sci. Ecotechnology 4, 100062. https://doi.org/10.1016/j.ese.2020.100062.

Hindatu, Y., Annuar, M.S.M., Gumel, A.M., 2017. Mini-review: Anode modification for improved performance of microbial fuel cell. Renew. Sust. Energ. Rev. 73, 236–248. https://doi.org/10.1016/j.rser.2017.01.138.

Korth, B., Rosa, L.F.M., Harnisch, F., Picioreanu, C., 2015. A framework for modeling electroactive microbial biofilms performing direct electron transfer. Bioelectrochemistry 106, 194–206. https://doi.org/10.1016/j.bioelechem.2015.03.010.

Lee, H.-S., Torres, C.I., Rittmann, B.E., 2009. Effects of substrate diffusion and anode potential on kinetic parameters for anode-respiring bacteria. Environ. Sci. Technol. 43, 7571–7577.

Lide, D., 2006. CRC Handbook of Chemistry and Physics, 87th ed. CRC Press, Cleveland.

Logan, B.E., Hamelers, B., Rozendal, R., Schröder, U., Keller, J., Freguia, S., Aelterman, P., Verstraete, W., Rabaey, K., 2006. Microbial fuel cells: methodology and technology. Environ. Sci. Technol. https://doi.org/10.1021/es0605016.

Lusk, B.G., Parameswaran, P., Popat, S.C., Rittmann, B.E., Torres, C.I., 2016. The effect of pH and buffer concentration on anode biofilms of Thermincola ferriacetica. Bioelectrochemistry 112, 47–52. https://doi.org/10.1016/j.bioelechem.2016.07.007.

Ly, H.K., Harnisch, F., Hong, S.F., Schröder, U., Hildebrandt, P., Millo, D., 2013. Unraveling the interfacial electron transfer dynamics of electroactive microbial biofilms using surface-enhanced raman spectroscopy. ChemSusChem 6, 487–492. https://doi.org/10.1002/cssc.201200626.

Marcus, A.K., Torres, C.I., Rittmann, B.E., 2007. Conduction-based modeling of the biofilm anode of a microbial fuel cell. Biotechnol. Bioeng. 98, 1171–1182. https://doi.org/10.1002/bit.

Molenaar, S.D., Sleutels, T., Pereira, J., Iorio, M., Borsje, C., Zamudio, J.A., Fabregat-Santiago, F., Buisman, C.J.N., Heijne, A.Ter, 2018. In situ biofilm quantification in bioelectrochemical systems by using optical coherence tomography. ChemSusChem 11, 2171–2178. https://doi.org/10.1002/cssc.201800589.

Pham, T.H., Rabaey, K., Aelterman, P., Clauwaert, P., De Schamphelaire, L., Boon, N., Verstraete, W., 2006. Microbial fuel cells in relation to conventional anaerobic digestion technology. Eng. Life Sci. 6, 285–292. https://doi.org/10.1002/elsc.200620121.

Pham, H.T., Boon, N., Aelterman, P., Clauwaert, P., De Schamphelaire, L., Van Oostveldt, P., Verbeken, K., Rabaey, K., Verstraete, W., 2008. High shear enrichment improves the performance of the anodophilic microbial consortium in a microbial fuel cell. Microb. Biotechnol. 1, 487–496. https://doi.org/10.1111/j.1751-7915.2008.00049.x.

Renslow, R.S., Babauta, J.T., Majors, P.D., Beyenal, H., 2013. Diffusion in biofilms respiring on electrodes. Energy Environ. Sci. 6, 595–607. https://doi.org/10.1039/c2ee23394k.

Sleutels, T., Darus, L., Hamelers, H.V.M., Buisman, C.J.N., 2011. Effect of operational parameters on Coulombic efficiency in bioelectrochemical systems. Bioresour. Technol. 102, 11172–11176. https://doi.org/10.1016/j.biortech.2011.09.078.

Sleutels, T., Molenaar, S., Heijne, A., Buisman, C., 2016. Low substrate loading limits methanogenesis and leads to high coulombic efficiency in bioelectrochemical systems. Microorganisms 4, 1–11. https://doi.org/10.3390/microorganisms4010007.

Sun, D., Chen, J., Huang, H., Liu, W., Ye, Y., Chen, S., 2016. The effect of biofilm thickness on electrochemical activity of Geobacter sulfurreducens. Int. J. Hydrog. Energy 41, 16523–16528. https://doi.org/10.1016/j.ijhydene.2016.04.163.

Sun, D., Cheng, S., Zhang, F., Logan, B.E., 2017. Current density reversibly alters metabolic spatial structure of exoelectrogenic anode biofilms. J. Power Sources 356, 566–571. https://doi.org/10.1016/j.jpowsour.2016.11.115.

ter Heijne, A., Schaetzle, O., Gimenez, S., Navarro, L., Hamelers, B., Fabregat-Santiago, F., 2015. Analysis of bio-anode performance through electrochemical

impedance spectroscopy. Bioelectrochemistry 106, 64–72. https://doi.org/10.1016/j.bioelechem.2015.04.002.

ter Heijne, A., Liu, D., Sulonen, M., Sleutels, T., Fabregat-Santiago, F., 2018. Quantification of bio-anode capacitance in bioelectrochemical systems using Electrochemical Impedance Spectroscopy. J. Power Sources 400, 533–538. https://doi.org/10.1016/j.jpowsour.2018.08.003.

Torres, C.I., Marcus, A.K., Lee, H.S., Parameswaran, P., Krajmalnik-Brown, R., Rittmann, B.E., 2010. A kinetic perspective on extracellular electron transfer by anode-respiring bacteria. FEMS Microbiol. Rev. 34, 3–17. https://doi.org/10.1111/j.1574-6976.2009.00191.x.

Villano, M., Ralo, C., Zeppilli, M., Aulenta, F., Majone, M., 2016. Influence of the set anode potential on the performance and internal energy losses of a methane-producing microbial electrolysis cell. Bioelectrochemistry 107, 1–6. https://doi.org/10.1016/j.bioelechem.2015.07.008.

Wanner, O., Gujer, W., 1986. A multispecies biofilm model. Biotechnol. Bioeng. 28, 314–328. https://doi.org/10.1002/bit.260280304.

Wanner, O., Ebert, H., Morgenroth, E., Noguera, D., Picioreanu, C., Rittmann, B., Van Loosdrecht, M.C.M., 2006. Mathematical Modeling of Biofilms.

Zhu, X., Yates, M.D., Logan, B.E., 2012. Set potential regulation reveals additional oxidation peaks of Geobacter sulfurreducens anodic biofilms. Electrochem. Commun. 22, 116–119. https://doi.org/10.1016/j.elecom.2012.06.013.